Chaos Dynamics in the Trajectory Control of Redundant Manipulators

Fernando B. M. Duarte

Dept. of Mathematics
Scholl of Technology, Polytechnic Institute of Viseu,
Viseu, Portugal

J. A. Tenreiro Machado

Dept. of Electrical Engineering
Institute of Engineering , Polytechnic Instit. of Porto
Porto, Portugal

Abstract

Several kinematic control algorithms for redundant manipulators adopt generalized inverse matrices. In this line of thought, the generalized inverse control scheme is tested through experiments that reveal the difficulties that often arise. Motivated by these problems this paper studies kinematics and dynamics of the trajectory planning scheme. The experiment confirm the non-linear and chaotic performance of the algorithm and gives a deeper insight towards the future development of superior trajectory control systems.

1 Introduction

A kinematically redundant manipulator is a robotic arm possessing more degrees of freedom (*dof*) than those required to establish an arbitrary position and orientation of the end effector [1, 2, 4]. When a manipulator is redundant, it is anticipated that the inverse kinematics admits an infinite number of solutions. This implies that, for a given location of the manipulator's end effector, it is possible to induce a self-motion of the structure without changing the location of the gripper. Thus, the arm can be reconfigured to find better postures for an assigned set of task requirements.

Many techniques for solving the kinematics of redundant manipulators that have been suggested control the end effector indirectly, through the rates at which the joints are driven, using the pseudoinverse of the Jacobian [3,15,16,17]. Nevertheless, these algorithms lead to a kind of chaotic motion with unpredictable arm configurations. Therefore, an important area of research remains open and more efficient algorithms must be envisaged.

Having these ideas in mind, the paper is organized as follows. Section 2 develops the formalism for the kinematics and dynamics of redundant manipulators. Based on these concepts, section 3 presents several experiments with the kinematics and dynamics of redundant robots. Section 4 analyses the chaotic phenomena revealed by the trajectory planning algorithms. Section 5 draws the main conclusions.

2 Kinematics And Dynamics Of Redundant Manipulators

2.1 Problem Formulation

We consider a manipulator with n *dof* whose joint variables are denoted by $\mathbf{q} = [q_1, q_2, ..., q_n]^T$. We assume that a class of tasks we are interested in can be described by m variables $\mathbf{x} = [x_1, x_2, ..., x_m]^T$ ($m < n$) and that the relation between $\mathbf{q}$ and $\mathbf{x}$ is given by:

$$\mathbf{x} = f(\mathbf{q}) \tag{1}$$

where f is a function representing the direct kinematics. Differentiating (1) with respect to time yields:

$$\dot{\mathbf{x}} = \mathbf{J}(\mathbf{q})\dot{\mathbf{q}} \tag{2}$$

where $\mathbf{J}(\mathbf{q}) = \partial f(\mathbf{q})/\partial \mathbf{q} \in \Re^{m \times n}$.

Several approaches for solving redundancy that have been proposed [5, 8] are based on the inversion of equation (2). A solution in terms of the joint velocities, is sought as:

$$\dot{\mathbf{q}} = \mathbf{J}^{\#}(\mathbf{q})\dot{\mathbf{x}} \tag{3}$$

where $\mathbf{J}^{\#}$ is one of the generalized inverses [6] of $\mathbf{J}$.

In the closed-loop pseudoinverse's method (CLP) the joint positions can be computed through the time integration of the velocities (3) according with the block diagram depicted in Figure 1.

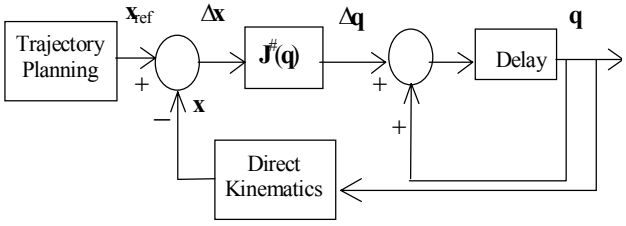

Fig. 1. Block diagram of the closed-loop inverse kinematics algorithm with the pseudoinverse.

An aspect revealed by the CLP is that repetitive trajectories in the operational space do not lead to periodic

trajectories in the joint space [7, 9]. This is an obstacle for the solution of many tasks because the resultant robot configurations have similarities with those of an chaotic system. To solve this lack of repetition several others methods were proposed. Nevertheless, clear conclusions about the nature of the phenomena involved when using $\mathbf{J}^{\#}$ are still lacking.

In order to compare performances with a 'non-chaotic' algorithm, in this paper we also consider an alternative trajectory planning approach, entitled Open-Loop Manipulability (OLM) optimization method [11,12,13,14]. For a given point in the operational space the algorithm consists on computing the point in the joint space that maximizes the manipulability index $\mu = \left(\det\left(\mathbf{J}\mathbf{J}^T\right)\right)^{1/2}$ [4,5]. Therefore, from the solution $\{q_1, \ldots, q_n\}$ we can extract a set of $n-m$ joint positions $\{q_j, \ldots, q_{j+n-m}\}$ optimal in a μ perspective. From these values and using a standard least squares method we calculate $n-m$ **x**-dependent polynomials that fit approximately the data. Once fixed these variables, the other m joint positions can be calculated through a standard inverse kinematic algorithm.

2.2 Kinematics and Dynamics

The direct kinematics and the Jacobian of a k-link planar manipulator has a simple recursive nature according with the expressions:

$$\begin{bmatrix} x \\ y \end{bmatrix} = \begin{bmatrix} l_1 C_1 + l_2 C_{12} + \cdots + l_k C_{1k} \\ l_1 S_1 + l_2 S_{12} + \cdots + l_k S_{1k} \end{bmatrix} \quad (4.a)$$

$$\mathbf{J} = \begin{bmatrix} -l_1 S_1 - l_2 S_{12} - \cdots - l_k S_{1k} \\ l_1 C_1 + l_2 C_{12} + \cdots + l_k C_{1k} \end{bmatrix} \quad (4.b)$$

where l_i is the length of link i, $S_{ik} = Sin(q_i + \cdots + q_k)$ and $C_{ik} = Cos(q_i + \cdots + q_k)$.

The symbolic formulae for the inverse dynamics of a k-link planar robot can be formulated recursively as:

$$\begin{aligned} T = & \sum_{i=1}^{n} (m_i (\sum_{p=1}^{i-1} (If\,[j > p, B1 = 0, B1 = 1], l_p{}^2 \sum_{u=1}^{p} \ddot{q}_u B1) \\ & + r_i{}^2 \sum_{u=1}^{i} \ddot{q}_u + \sum_{p=2}^{i} (\sum_{k=1}^{p-1} (If\,[p > i-1, B2 = 0, B2 = 1], \\ & [If\,[p == i, B3 = 1, B3 = 0]], If\,[j > k, B4 = 0, B4 = 1], \\ & If\,[(j >= k+1 \,\&\&\, j <= p), B5 = 1, B5 = 0], \\ & l_k (l_p B2 + r_p B3)((-S_{k+1..p} ((\sum_{u=k+1}^{p} \dot{q}_u)^2 + \\ & 2 \sum_{u=1}^{k} \dot{q}_u \sum_{u=k+1}^{p} \dot{q}_u) + C_{k+1..p} (\sum_{u=1}^{p} \ddot{q}_u + \sum_{u=1}^{k} q_u))) B4 + \\ & (S_{k+1..p} (\sum_{u=1}^{k} \dot{q}_u)^2 + C_{k+1..p} \sum_{u=1}^{k} \ddot{q}_u) B5 + \\ & g (\sum_{p=1}^{i-1} (If\,[j > p, B1 = 0, B1 = 1], l_p C_{1..p} B1) + r_i C_{1..i}))) \end{aligned} \quad (5)$$

where T are the joints torques $B1$ to $B5$ are logical conditions, m_i is the mass of link i, r_i is the distance from the joint axis to the link center of mass and g is the acceleration due to gravity.

During the experiments, it is considered $\Delta t = 0.00$ sec, $l_1 + l_2 + \ldots + l_k = 3$, $l_1 = l_2 = \ldots = l_k$, $m_1 + m_2 + \ldots + m_k = 3$, and $m_1 = \ldots = m_k$.

3 Trajectory Control Of Redundant Manipulators

In this section we analyze the performances of the trajectory controllers based on the CLP and OLM methods. In this line of thought, we study the joint trajectories for the redundant 3R robot, when subjected to a repetitive circular trajectory in the operational space with radius ρ.

In a first set of experiments we adopt the 3R arm with an initial posture $\mathbf{q}(0) = [\pi \quad -\pi/2 \quad -\pi/2]^T$. Figure 2 and 3 show the joint positions for the CLP and OLM methods, respectively. In the OLM algorithm it is adopted the least square approximation polynomial $q_3 = 0.51r - 2.09$ for joint 3, where $r = \left(x^2 + y^2\right)^{1/2}$.

In these two experiments we have distinct results. When adopting the CLP, the manipulability is non-optimal and the joint trajectories exhibit sudden changes, which impose large joint velocities. Moreover, the joint trajectories are non-repetitive leading to a kind of chaotic performance. When using the OLM procedure the trajectory is repetitive without large or fast transients.

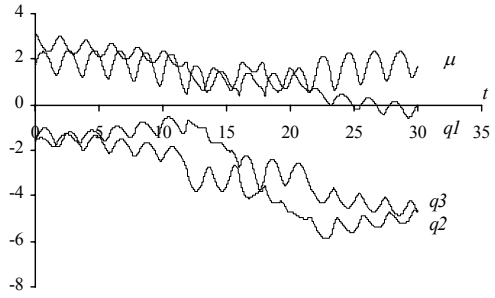

Fig. 2. The 3R-robot joint positions *versus* time using the CLP method for $r = 1$, $\rho = 0.5$.

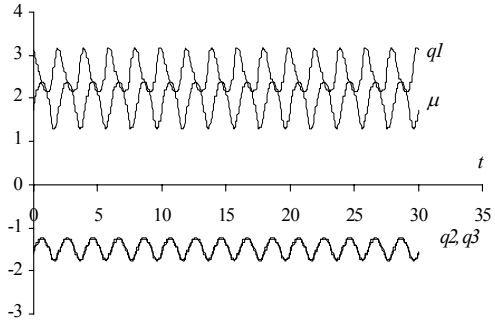

Fig.3. The 3R-robot joint positions *versus* time using the OLM method for $r = 1$, $\rho = 0.5$.

In a second set of experiments we analyze the robot inverse dynamics when subjected to the repetitive circular trajectory in the operational space. Figure 4 shows the resulting the joint torque for the 3*R* manipulator when the CLP method is used. It is clear that the dynamics follows the kinematic non-repetitive responses and, therefore, exhibits the same type of problems.

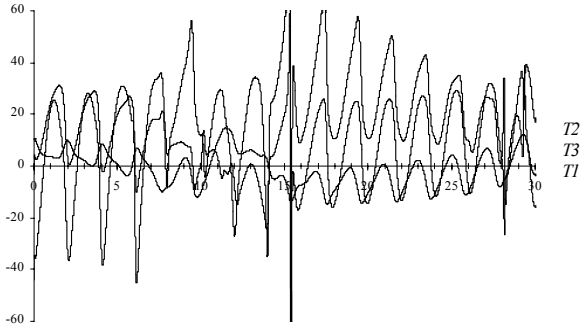

Fig. 4. The 3*R*-robot joint torques *versus* time using the CLP method ($r = 1$, $\rho = 0.5$). The joint 1 maximum torque is T_1=158.1 *Nm* at *t=15.3 sec*. The joint 2 maximum torque is T_2=67.6 *Nm* at *t=15.3 sec*. The joint 3 maximum torque is T_3=14.7 *Nm* at *t=11.5 sec*.

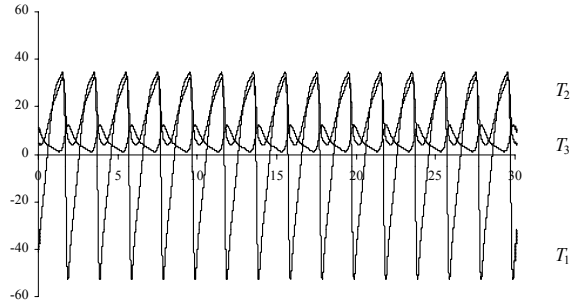

Fig. 5. The 3*R*-robot joint torques *versus* time using the OLM method ($r = 1$, $\rho = 0.5$).

On the other hand, Figure 5 shows the resulting joint torques for the 3*R* manipulator using the OLM method. As expected, with this method the dynamics is repetitive without fast, high-amplitude transients.

4 Analyzing The Chaotic-Like Responses Of The Pseudoinverse Algorithm

It was shown previously that the pseudoinverse algorithm leads to unpredictable arm configurations, with responses similar to those of a chaotic system [13,14].

For example, Figures 6 - 9 depict the phase-plane joint trajectories for the 3*R*-robot positions and torques, respectively, when repeating a circular motion, with center at $(x, y) = \left(\sqrt{2}/2, \sqrt{2}/2\right)$ and radius $\rho = 0.1$, under the CLP and OLM schemes. For the CLP method, besides the motion drift, leading to different trajectory loops, we have points that are 'avoided'. Such points correspond to arm configurations where several links are aligned. This characteristic is inherent to the pseudoinverse matrix, because the 3*R*-robot was tested both under open-loop and closed-loop control, leading to the same type of behavior. In order to gain further insight into the chaotic nature of the phenomena, the robots under investigation were required to follow the cartesian repetitive circular motion for several radial distances (r). The phase-plane joint trajectories were then analyzed and their fractal dimension (*dim*) estimated through the standard box-counting method:

$$\dim S = \lim_{\varepsilon \to 0} \frac{\ln N(\varepsilon)}{\ln (1/\varepsilon)} \qquad (6)$$

where $N(\varepsilon)$ denotes the smallest number of bi-dimensional boxes of side length ε required in order to completely cover the plot surface S [10].

The results, according with Figure 10, show that:

- for the pseudoinverse method we have *dim* ≈ 2 due to the position and velocity drifts, in contrast with the 'standard' case where we have *dim* ≈ 1.
- the fractal dimension diminishes near the maximum radial distance (*i.e.* $r = 3$).
- for each type of robot the fractal dimension is nearly the same, for all joints.
-

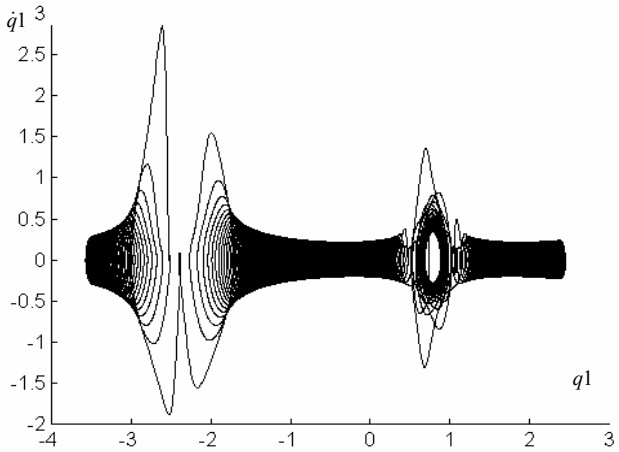

Fig. 6. Phase plane $\{q_1, \dot{q}_1\}$ trajectory for the 3*R*- robot joint 1 under CLP method at $r = 1$, $\rho = 0.1$, *dim* = 1.62.

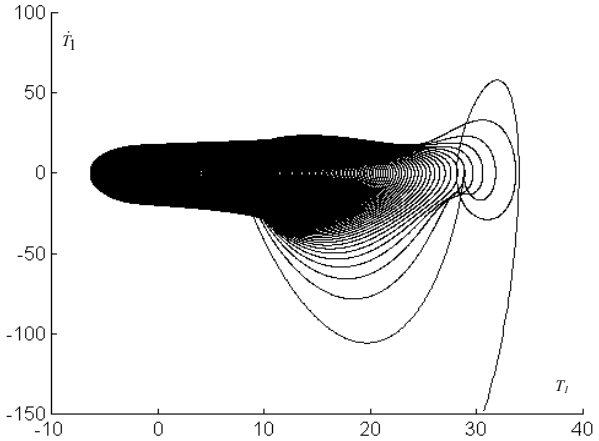

Fig. 7. Phase plane $\{T_1, \dot{T}_1\}$ trajectory for the 3*R*- robot torque 1 under CLP method at $r = 1$, $\rho = 0.1$, *dim* = 1.69.

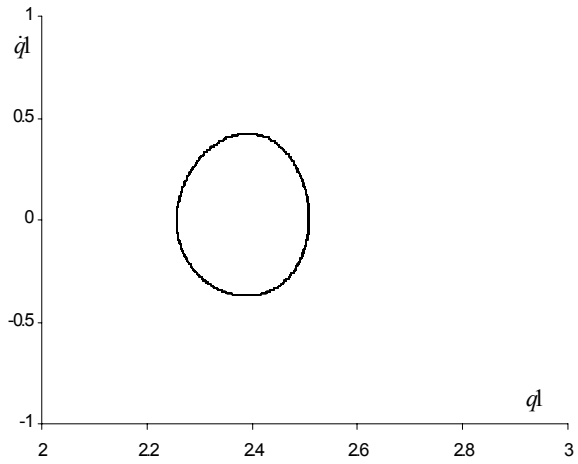

Fig. 8. Phase plane $\{q_1, \dot{q}_1\}$ trajectory for the 3*R*- robot joint 1 under OLM method at $r = 1$, $\rho = 0.1$, $dim = 1$.

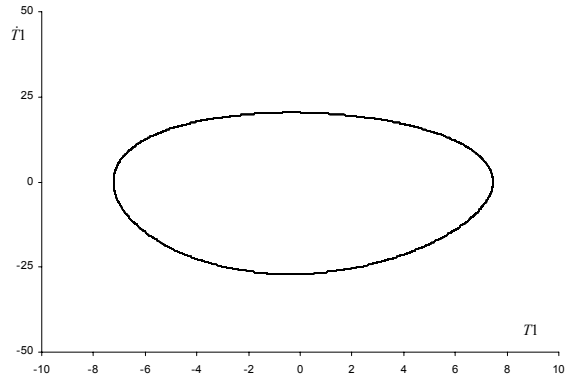

Fig. 9. Phase plane $\{T_1, \dot{T}_1\}$ trajectory for the 3*R*- robot torque 1 under OLM method at $r = 1$, $\rho = 0.1$, $dim = 1$.

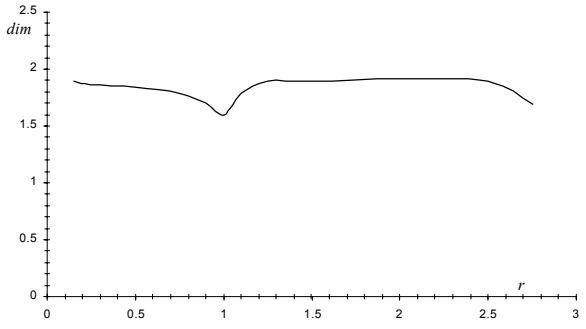

Fig. 10. Fractal dimension *dim* of the kinematic phase-plane *versus* the radial distance *r* for the 3*R* ($\rho = 0.1$) with de CLP method.

The robot chaotic motion is due to the contribution of the Jacobian pseudoinverse to the manipulator inner motion. Nevertheless, a deeper insight into the nature of this motion must be envisaged. Therefore, two distinct experiments were devised to establish the texture of the Jacobian null space.

In a first experiment, the robot is required to start in an initial random configuration with $q_i \in]-\pi,\pi]$ ($i = 1, 2, 3$) and to attain a fixed point in the operation space under the control of the CLP scheme. After elapsing the trajectory transient, the final robot joint positions are recorded. The experiment is repeated in order to establish a statistical characterization of the manipulator steady-state configuration. Figure 11 shows a typical histogram for the 3*R* robot joint positions. For a given desired position in the operational space, we conclude that the possible robot configurations have distinct probabilities. In this perspective, Figure 12 shows the variation of the most probable q_i ($i = 1, 2, 3$) *versus* the radial distance *r* (for $x = r$ and $y = 0$).

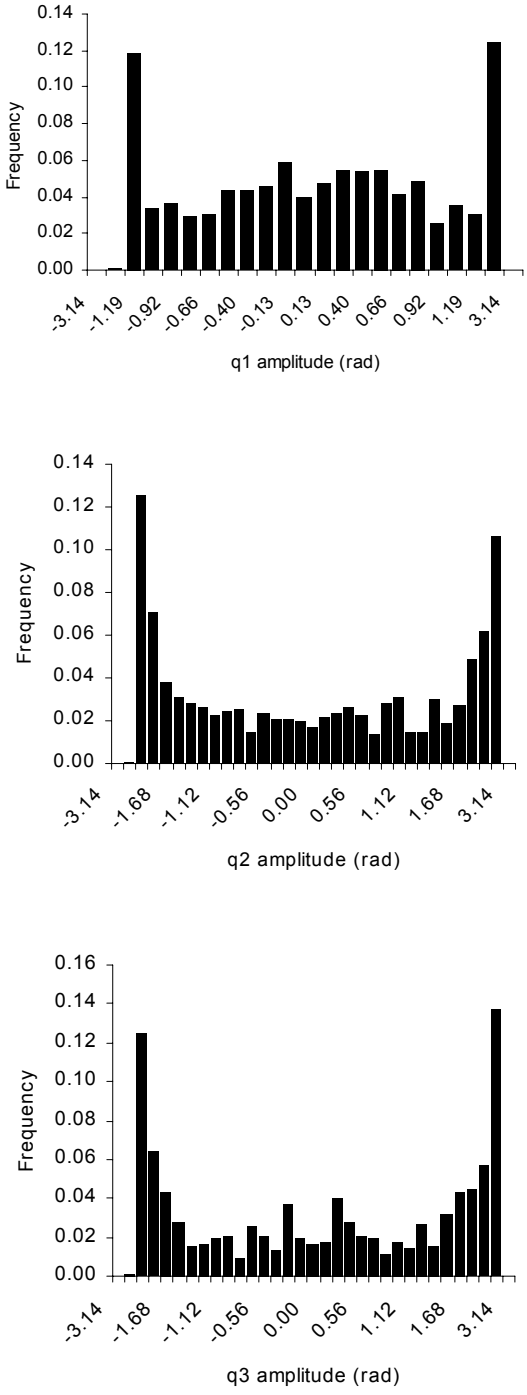

Fig. 11. Histogram for the 3*R* robot joint positions, with final gripper position: $(x, y) = (\sqrt{2}, \sqrt{2})$.

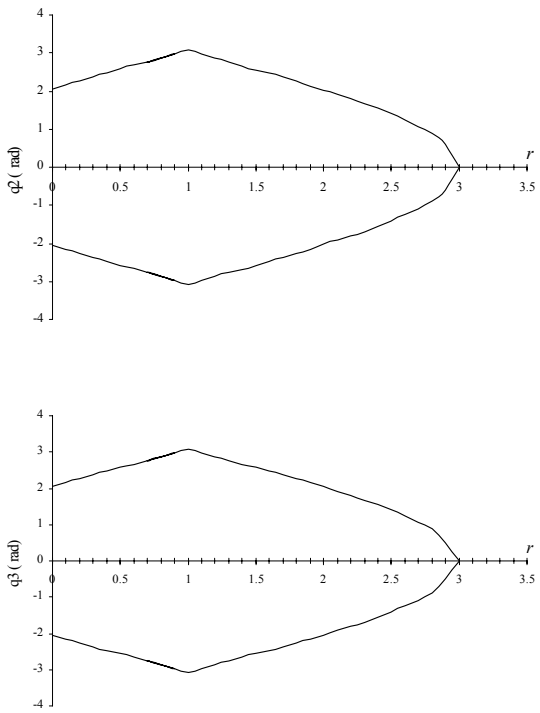

Fig. 12. Most probable robot joint positions *vs* the radial distance *r*.

In a second set of experiments the frequency response of the CLP method for the 3*R* robot was computed numerically. Figure 13 depict the resulting amplitude Bode diagrams for $r = 2$ and $\rho \in \{0.10, 0.25, 0.50, 0.75, 1.00\}$ for the CLP scheme.

It is clear that the transfer matrix for the *MIMO* system $(x_{ref}, y_{ref}) \rightarrow (q_1, q_2, q_3)$ depends strongly on the amplitude of the 'exciting' signal ρ. Moreover, the Bode diagrams reveal that the CLP method presents distinct gains for the joint variables, according with the frequency.

This conclusion is consistent with the phase-plane charts, that revealed low frequency drifts, while responding to an higher frequency signal input.

On the other hand, the OLM method shows a minor gain variation with ω as shown in Figure 14, which agrees with the phase-plane portrait studied previously.

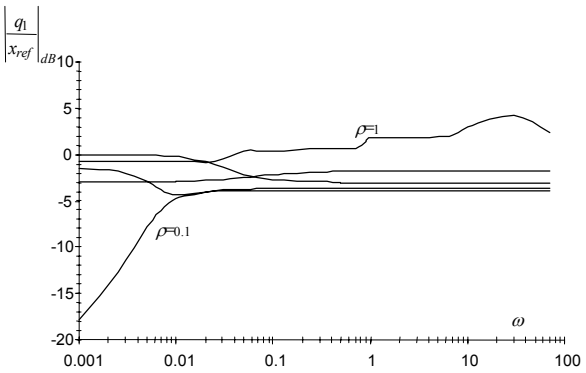

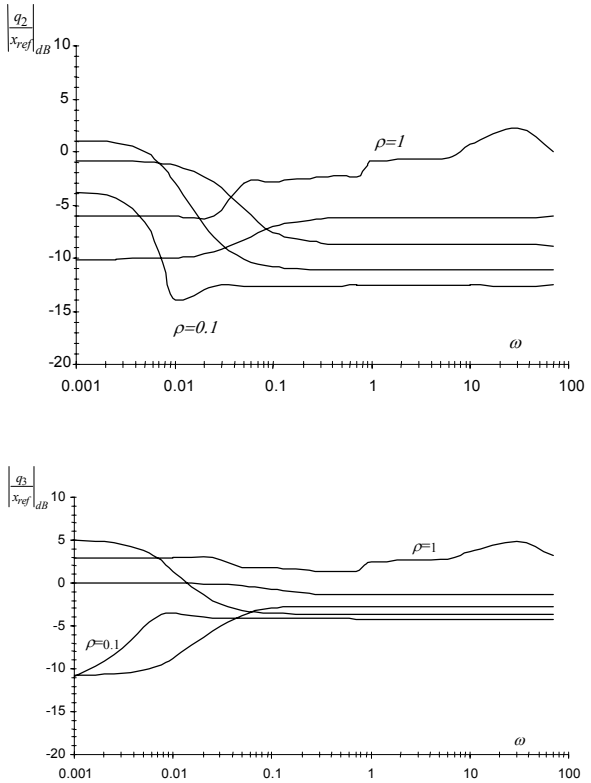

Fig. 13. Frequency response of the CLP method for the 3*R* robot, $r = 2$, $\rho \in \{0.10, 0.25, 0.50, 0.75, 1.00\}$

5 Conclusions

This paper discussed several aspects of the phenomena generated by the pseudoinverse-based trajectory control of redundant manipulators. An alternative based on the least squares polynomial approximation to the manipulability optimization was also presented. Furthermore, the study addressed both the kinematics and dynamics in order to test the influence of each model.

These techniques were applied in the trajectory control of redundant manipulators and their characteristics compared. The CLP scheme leads to non-optimal responses, both for the manipulability and the repeatability perspectives while the OLM method revealed superior performances.

The fractal dimension of the responses was analyzed showing that it is independent of the robot joint. In fact, the chaotic motion depends on the operational space point and on the amplitude of the exciting repetitive motion. In this perspective, the chaotic responses where analyzed from different point of views namely, phase-plane, statistics and frequency response. The results are consistent and represent a step towards the development of superior trajectory planning algorithms for redundant manipulators.

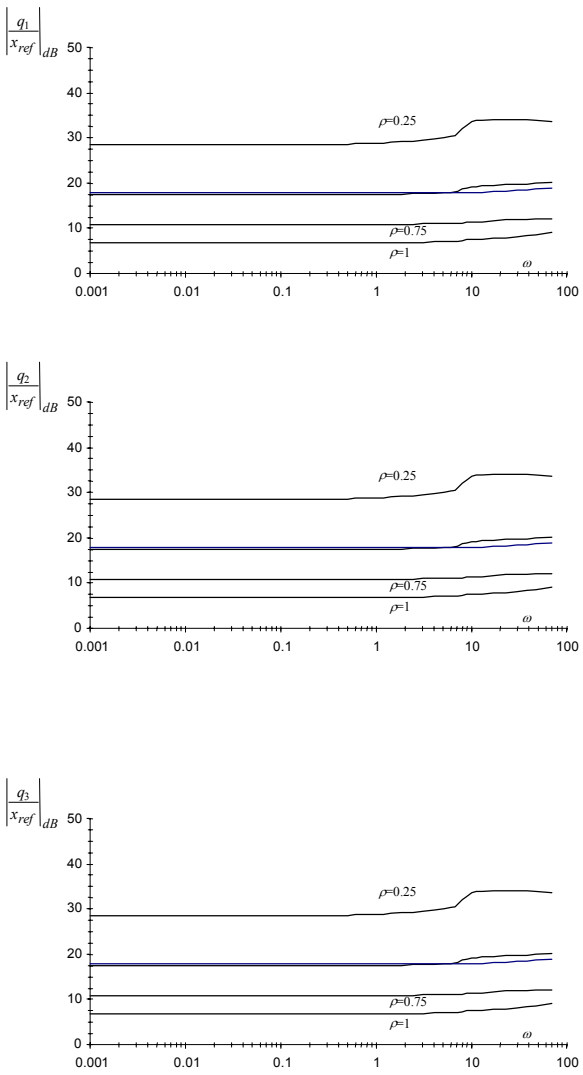

Fig. 14. Frequency response of the CLP method for the $3R$ robot, $r = 2$, $\rho \in \{0.10, 0.25, 0.50, 0.75, 1.00\}$

References

[1] E. Sahin Conkur, And Rob Buckingham "Clarifying the Definition of Redundancy as Used in Robotics", *Robotica*, vol. 15, pp. 583-586, 1997.

[2] Stefano Chiaverini "Singularity-Robust task-Priority Redundancy Resolution for Real Time Kinematic Control of Robot Manipulators", *IEEE Transactions Robotics Automation*, vol. 13, pp. 398-410, 1997.

[3] C.A Klein, and C. C Huang, "Review of Pseudoinverse Control for Use With Kinematically Redundant Manipulators", *IEEE Trans. Syst. Man, Cyber.*, vol. 13, pp. 245-250, 1983.

[4] Yoshikawa, T., "*Foundations of Robotics: Analysis and Control*", MIT Press, 1988.

[5] Y. Nakamura, "*Advanced Robotics: Redundancy and Optimization*", Addinson-Wesley, 1991.

[6] Keith L. Doty, C. Melchiorri and C. Bonivento, "A Theory of Generalized Inverses Applied to Robotics", *International Journal of Robotics Research*, vol. 12, pp. 1-19, 1993.

[7] Bruno Siciliano, " Kinematic Control of Redundant Robot Manipulators: A Tutorial", *Journal of Intelligent and Robotic Systems*, vol. 3, pp. 201-212, 1990.

[8] W.J.Chung, Y. Youm and W. K. Chung, "Inverse Kinematics of Planar Redundant Manipulators via Virtual Links With Configuration Index", *Journal of Robotic Systems*, vol. 11, pp. 117-128, 1994.

[9] Sanjeev Seereeram and John T. Wen, "A Global Approach to Path Planning for Redundant Manipulators", *IEEE Transactions Robotics Automation*, vol. 11, pp.152-159, 1995.

[10] James Theiler, "*Estimating Fractal Dimension*", *Journal Optical Society of America*, vol. 7, nº6, pp. 1055-1073, 1990.

[11] Fernando B.M. Duarte and J.A. Tenreiro Machado, "Kinematic Optimazition of Redundant and Hyper-Redundant Robot Trajectories", ICECS'98-5th IEEE International Conference on Electronics, Circuits and Systems, Lisbon, Portugal, 1998.

[12] J.A.Tenreiro Machado and Fernando B. Duarte, "Redundancy Optimization for Mechanical Manipulators", *AMC'98*-5th IEEE International Workshop on Advanced Motion Control, Coimbra, Portugal, 1998.

[13] Fernando B. Duarte and J.A. Tenreiro Machado, "Chaotic Phenomena and Performance Optimization in the Trajectory Control of Redundant Manipulators", in *Recent Advances in Mechatronics*, Springer-Verlag, Eds O. Kaynak et al., 1999.

[14] Fernando B. Duarte and J.A. Tenreiro Machado, "On the Optimal Configuration of Redundant Manipulators", INES'98- 9th IEEE Int. Conf. on Intelligent Engineering Systems, Vienna, Austria, 1998.

[15] R. G. Roberts and A. A. Maciejewski, "Singularities, Stable Surfaces and the Repeatable Behaviour of Kinematically Redundant Manipulators", *International Journal of Robotics Research*, vol. 13, nº 1, pp. 70-81, 1994.

[16] R. G. Roberts and A. A. Maciejewski, "Repeatble Generalized Inverse Control Strategies for Kinematically Redundant Manipulators", *IEEE Transactions on Automatic Control*, vol. 38, nº 5, pp. 689-699, 1993.

[17] J. S. Bay, "Geometry and Prediction of Drift-Free Trajectories for Redundant Machines Under Pseudoinverse Control", *International Journal of Robotics Research*, vol. 11, nº 1, pp. 41-52, 1992.